Optics & Laser Technology 134 (2021) 106657

Contents lists available at ScienceDirect

Optics and Laser Technology

journal homepage: www.elsevier.com/locate/optlastec

Full length article

Picosecond high-power 213-nm deep-ultraviolet laser generation using β-BaB_2O_4 crystal

Yuxi Chu [a], Xudong Zhang [a], Binbin Chen [b], Jiazan Wang [b], Junhong Yang [c], Rui Jiang [b,d], Minglie Hu [a,*]

[a] Ultrafast Laser Laboratory, Key Laboratory of Opto-electronic Information Science and Technology of Ministry of Education, School of Precision Instruments and Opto-electronics Engineering, Tianjin University, 300072 Tianjin, China
[b] Beijing RS Laser Opto-Electronics Technology CO., Ltd, 100176 Beijing, China
[c] Key & Core Technology Innovation Institute of the Greater Bay Area, 510670 Guangdong, China
[d] Institute of Microelectronics of the Chinese Academy of Science, 100029 Beijing, China

ARTICLE INFO

Keywords:
High power
Picosecond
Fifth-harmonics generation
Deep-ultraviolet

ABSTRACT

In this study, we successfully demonstrate the achievement of 1.37 W average power for a picosecond deep ultraviolet (DUV) laser at 213 nm with a 1 MHz repetition rate using β-BaB_2O_4 (BBO) crystals, which is the highest output power of a 213 nm picosecond laser system with an all-solid-state setup so far. The laser system generates over 1.3 μJ 213-nm pulse energy. The fifth harmonic is generated by sum-frequency generation of the 532 and 355 nm beams based on a "2 + 3" scheme. BBO crystals with lengths of 6, 8, and 10 mm are investigated. Furthermore, the DUV laser system produces a high-beam quality and narrow linewidth output. The DUV system can be stably maintained over 100 h with expanded beam sizes of 532 and 355 nm at 800 mW, and without requiring a change in the positions and temperatures of nonlinear crystals.

1 Introduction

To date, high-power and high-repetition rate deep ultraviolet (DUV) laser sources, with pulse lengths in picosecond regions, have been widely applied in both science and industry, including online detection of wafer surface defects, laser drilling, laser machining of wide bandgap materials, and research on surface physics [1–3]. In recent years, due to the fast development of solid-state lasers and nonlinear optical crystals (NLO), high-energy, nanosecond-class DUV pulse, and continuous-wave lasers have been studied by many research groups [4–10]. These DUV lasers are typically generated by the fifth-harmonics generation (5HG) of near-infrared (NIR) lasers at 1 μm. For the DUV picosecond operations around 200-nm lasers that are subject to energies lower than those of the nanosecond pulses, the damage and impact of temporal walk-off effects, high power with high-energy operations have encountered serious beam deterioration, power reductions, and instabilities caused by DUV absorptions [11–14]. For the frequency conversions of visible and DUV radiation, birefringent crystals are crucial; thus, some properties, such as a DUV transparency of considerably less than 300 nm, moderate nonlinear coefficients (d_{eff} = 1–2 pm/V), high optical damage thresholds, and low cost, are important considerations.

Hitheto, the major 5HG NLO crystals include β-BaB_2O_4 (BBO), $CsLiB_6O_{10}$ (CLBO), $NH_4H_2PO_4$ (ADP), and KH_2PO_4 (KDP). ADP and KDP crystals can be grown in meter scale sizes, and the 20%-efficient 5HG of wide-aperture neodymium glass is first reported in an ADP crystal [15]. Also, both KDP and ADP crystals must be cooled to cryogenic temperatures to achieve phase-matching conditions. The 5HG is achieved at room temperature using BBO and CLBO. The CLBO crystal has been proved to be an attractive NLO crystal for generating DUV radiation owing to its larger angular acceptance, phase-matching bandwidth, and temperature bandwidth constants compared with those of BBO. Nonetheless, BBO and CLBO crystals can both be used to generate 213-nm wavelengths, as exemplified in Table 1 [16,17]. However, CLBO crystals can only be used in a "1 + 4" scheme through a sum-frequency generation of 1064 and 266 nm beams. CLBO crystals are generally used in picosecond 266-nm lasers [18,19]. In picosecond 266-nm lasers, high-power, long-term stability, and high-beam quality operations have to be through intermittent crystal shifting. For the generation of 213 nm based on the "1 + 4" scheme, the performances of the whole system are limited by the two processes of 266 and 213 nm, particularly for long-

* Corresponding author.
E-mail addresses: jiangrui@ime.ac.cn (R. Jiang), huminglie@tju.edu.cn (M. Hu).

https://doi.org/10.1016/j.optlastec.2020.106657
Received 10 April 2020; Received in revised form 29 September 2020; Accepted 5 October 2020
Available online 10 October 2020
0030-3992/© 2020 Elsevier Ltd. All rights reserved.

Table 1
Laser generation schemes for CLBO and BBO crystals at 213 nm.

	Schemes	Phase-matching angle (θ)	d_{eff} (pm/V)	Walk-off angle (°)	Crystal angle tolerance (mrad cm)
CLBO	1 + 4 (o + o → e)	67.6°	0.95	1.7	0.42
BBO	2 + 3 (o + o → e)	69.7°	1.1	3.5	0.21

term stability. Furthermore, CLBO crystal is known to be easily deliquescent because of its highly hygroscopic nature [20]. In contrast, BBO crystals can use a "2 + 3" scheme through a sum-frequency generation of easily obtainable 532 and 355 nm beams. So far, the lifetime and beam quality of 532 and 355 nm are sufficiently mature to support a 213-nm laser generation. However, BBO crystals suffer from two-photon absorption (TPA) during the 5HG, which seriously decreases the conversion efficiency and degrades the beam quality [21]. Meanwhile, the TPA coefficient β is a function of intensity. If the intensity is relatively low, typically below 10 MW/cm^2, then the contribution of TPA is weak [22]. Furthermore, as one of the most important NLO crystals, BBO has many outstanding features such as high NLO coefficients, low group-velocity dispersion, and high optical quality. BBO is also commercially available at a competitive price. Therefore, the generation of a picosecond "2 + 3" scheme based on BBO crystals at 213 nm is of great importance. High power of 1.15 [10] and 0.5 W [11] at 213 nm have been obtained by CLBO and BBO operating at 82 and 120 MHz respectively, but the DUV outputs produce with the lower pulse energy (nJ level) are not compatible with some applications when considering both the average and peak power.

In this study, we have designed an efficient 5HG system based on a "2 + 3" scheme, which cascades through a second harmonic generation (SHG) and a third harmonic generation (THG) both using LiB_3O_5 (LBO) as the nonlinear material and a BBO crystal in the 5HG process. To reduce the influence of TPA, a beam expander is inserted between THG and 5HG to increase the beam size and reduce the divergence angle at 532 and 355 nm. The maximum output power is as high as 1.37 W for a 213-nm wavelength at a 1 MHz repetition rate. The energy of the generated 213-nm pulse is over 1.3 μJ. We also investigate the influence of BBO crystal length on the 5HG output power, and the spectral evolution at 532, 355, and 213 nm. The long-term operation over 100 h is achieved at 800 mW, and no intermittent crystal shifting is required. Also, the DUV laser system produces a high-beam quality and narrow linewidth output.

2 Experiment setup

A schematic diagram of the experimental setup is shown in Fig. 1. A high-power diode-directly-pumped passively mode-locked Nd: YVO_4 solid-state laser was used as the pump source. An acousto-optic modulator (AOM) was applied to reduce the repetition rate of the seed pulses from 50 to 1 MHz. The picosecond laser amplifier consisted of dual-pass amplifier and a two-stage single-pass amplifier based on Nd: YVO_4 bulk crystals. The maximum power output was 50 W. A pair of lenses, L1 and L2, was used to adjust the pump beam size to approximately 2.2 mm in diameter. The LBO for the first SHG (LBO [1]) had dimensions of 5 mm × 5 mm × 20 mm, cut at θ = 90.0° with φ = 10.4°, and it was designed to type-I phase match at 50 °C. The LBO for the THG (LBO [2]) had dimensions 5 mm × 5 mm × 18 mm, cut at θ = 44.0° with φ = 90°. LBO (2) was designed for type-II phase-matching at 50 °C. The entrance face of LBO (2) was antireflection coated at 1064 and 532 nm, while the exit face of LBO (2) was antireflection coated at 1064, 532, and 355 nm. To compensate for the walk-off effect, the SHG was type-I phase matched at the XY plane and THG was type-II phase matched at the YZ plane, and the walk-off directions during SHG and THG were opposite [6]. The wavelengths at 532 and 355 nm were separated by a dichroic mirror (DM1) and another dichroic mirror (DM2) was used to separate 1064 nm. A half-wave waveplate was used to change the polarization at 532 nm to achieve the type-I phase-matching in 5HG BBO. A delay line was used to compensate for the temporal walk-off effect. A dichroic mirror (DM3) was used to combine 532 and 355 nm in space for BBO in 5HG. The surfaces of BBO in 5HG were all uncoated to avoid damage caused by deep-violet photons. A beam expander with a fixed magnification of 2× was inserted before 5HG. The beam expander has two functions. Firstly, not only can the efficiency of SHG and THG be guaranteed but also the peak power density at 532 and 355 nm can be reduced to avoid the damage of 5HG BBO crystal. The beam diameter after the expansion is about 2.7 and 2.0 mm at 532 and 355 nm, respectively. Secondly, the divergence angle at 532 and 355 nm can be reduced by twice. The lower divergence is beneficial for the generation of 213 nm because the BBO crystal has lower angular acceptance bandwidth compared with CLBO crystal. The divergence angle at 532 nm after the expansion is about 0.29 and 0.26 mrad in the x and y directions, respectively. The divergence angle at 355 nm after the expansion is about 0.20 and 0.19 mrad in the × and y directions, respectively.

3. Experiment results

The fundamental beam system is optimized to a high-beam quality at 1 MHz. Fig. 2 illustrates the measured pulse length of the fundamental

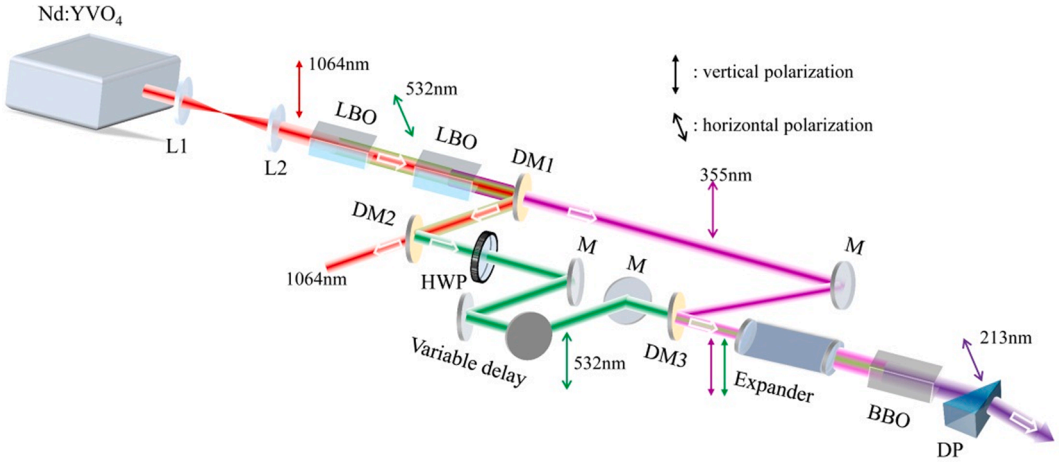

Fig. 1. A schematic diagram of the experimental setup for laser generation in BBO at 213 nm. L1, L2, focusing lenses; DM1, DM2, DM3 dichroic mirrors; HWP, half-wave waveplate; DP, CaF_2 dispersion prism.

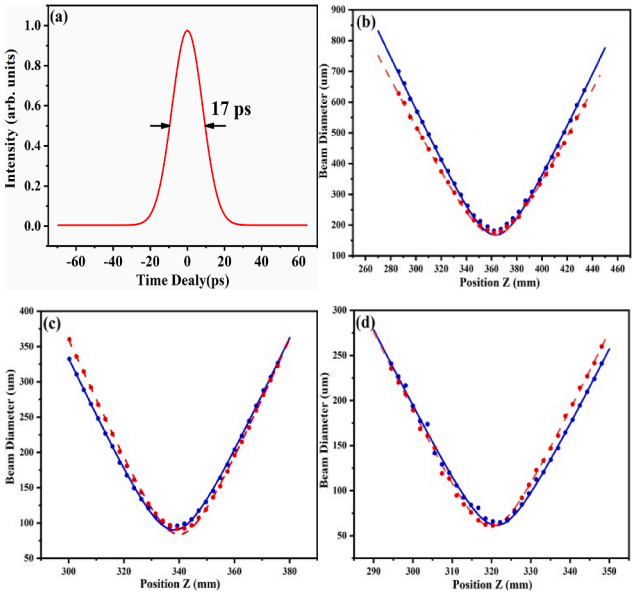

Fig. 2. Pulse length of the fundamental beam (a), M^2 factors (blue solid line: fitting horizontal diameters after lens, red dashed line: fitting vertical diameters after lens) of 1064 nm (b), 532 nm(c), and 355 nm (d). (For interpretation of the references to colour in this figure legend, the reader is referred to the web version of this article.)

beam at 50 W by an intensity autocorrelator (Pulse Check 150, APE), M^2 factors (BEAMAGE-M2, Gentec-EO). The pulse duration of fundamental beam is 17 ps. The values of M^2 are $M_x^2 = 1.08$ and $M_y^2 = 1.05$ at 1064 nm, $M_x^2 = 1.12$ and $M_y^2 = 1.1$ at 532 nm, $M_x^2 = 1.2$, and $M_y^2 = 1.17$ at 355 nm. The power stability of 1064, 532, and 355 nm is 0.48%, 0.63%, and 1.14% RMS respectively, over a 1-h measurement.

To prevent damage to the BBO crystal, we limit the maximum power output at 1064 nm to be 30 W. The SHG and THG conversion efficiencies are adjusted by changing the temperature of the LBO (1) and LBO (2) crystals to optimize the conversion efficiency at 213 nm. The maximum conversion efficiency is measured for a power ratio of 1:1 between 532 and 355 nm for the 10-mm BBO crystal. The resulting powers at 532 and 355 nm are measured to be about 8.0 W and 8.0 W respectively. The estimated peak intensity of 532 and 355 nm on the entrance face of the BBO crystal is 25 and 35 MW/cm^2, respectively. Three BBO crystals used in 5HG with lengths of 6, 8, and 10 mm are investigated, with the experimental results shown in Fig. 3 (a). Fig. 3 (a) shows the output power at 213 nm as a function of the input power at 532 nm. The 1064 nm power is fixed at 30 W and the power ratio between 532 and 355 nm is 1:1 during the whole process. The maximum output power at 213 nm is obtained from the 10 mm crystal having an output power of 1.37 W after a CaF_2 dispersion prism. The measured 213 nm power of 1.37 W is ~ 20% lower than the simulated result using SNLO. In Ref [12], the powers of 532 and 355 nm should be very low when the power of 1064 nm is low. Therefore, the much higher output powers are obtained in Fig. 3 (a) at low pump powers compared with the results of Ref [12]. Compared with Ref [13], the peak intensities of both input beams are much lower; no conversion efficiency saturation is observed, as shown in Fig. 3(b). The conversion efficiency is defined as the ratio of 213-nm output power to the 532-nm power at the input of the BBO crystal. Although the output power from the 10-mm crystal is higher than that from the 8-mm crystal, the beam profile at 213 nm from the 10-mm crystal is worse because the self-heating process caused by TPA and the subsequent thermal dephasing due to the small temperature acceptance of BBO is more serious for the longer crystal, as shown in the insets of Fig. 3 (a). The maximum output power at 213 nm is 1.16 W from the 8 mm-crystal after a CaF_2 dispersion prism, and near-field beam profile is with high quality. Fig. 4 shows the M^2 factors at 213 nm for the 8-mm

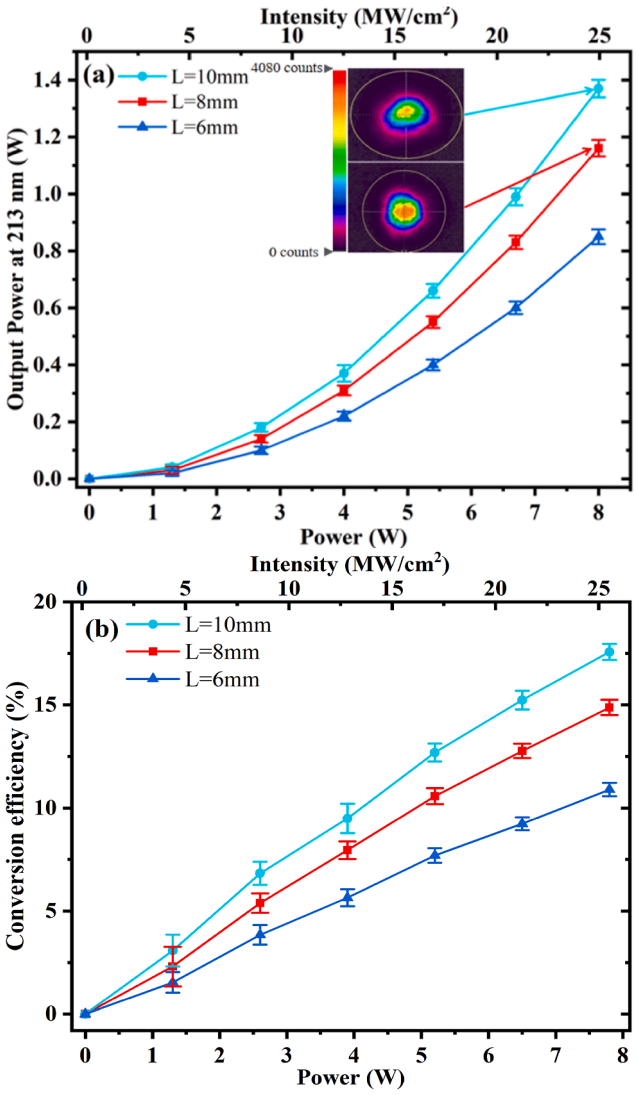

Fig. 3. Output power (a) and conversion efficiency (b) versus input power at 532 nm of the three BBO crystals used for 5HG. The inserts show beam profiles at 213 nm for 8 and 10 mm, respectively. Error bars represent the standard deviation over a number of measurements.

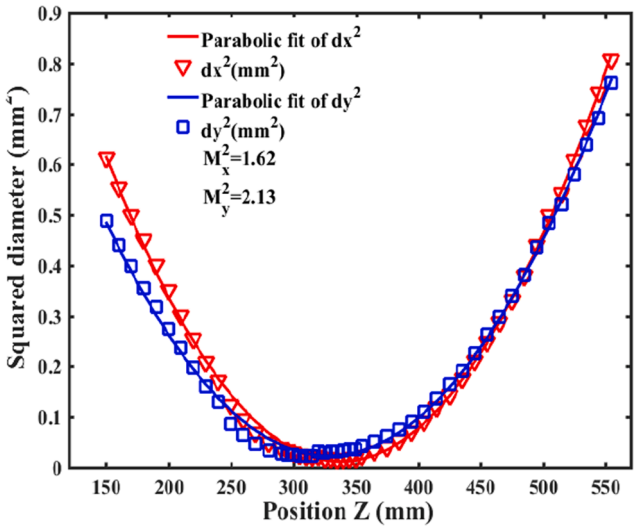

Fig. 4. M^2 factors of 213 nm for the 8 mm BBO crystal.

BBO crystal, $M_x^2 = 1.62$ and $M_y^2 = 2.13$.

Fig. 5 shows the spectral evolution at 532, 355, and 213 nm. A wavelength meter (ELIAS-Wavemeter, LTB) is used to measure the spectral width. The spectral shape of the 532 nm beam is attributed to the depletion during the THG process. Theoretically, the spectral width at 1064 nm is approximately 98.0 pm for the full width at half maximum (FWHM) based on the Fourier transform limit, while the spectral width at 532, 355, and 213 nm is 94, 88, and 14 pm (~90 GHz) for the FWHM, respectively. The measured spectral widths are larger than simulations by using the SNLO computer program. The linewidth of 213 nm is narrow enough for the wafer inspection process.

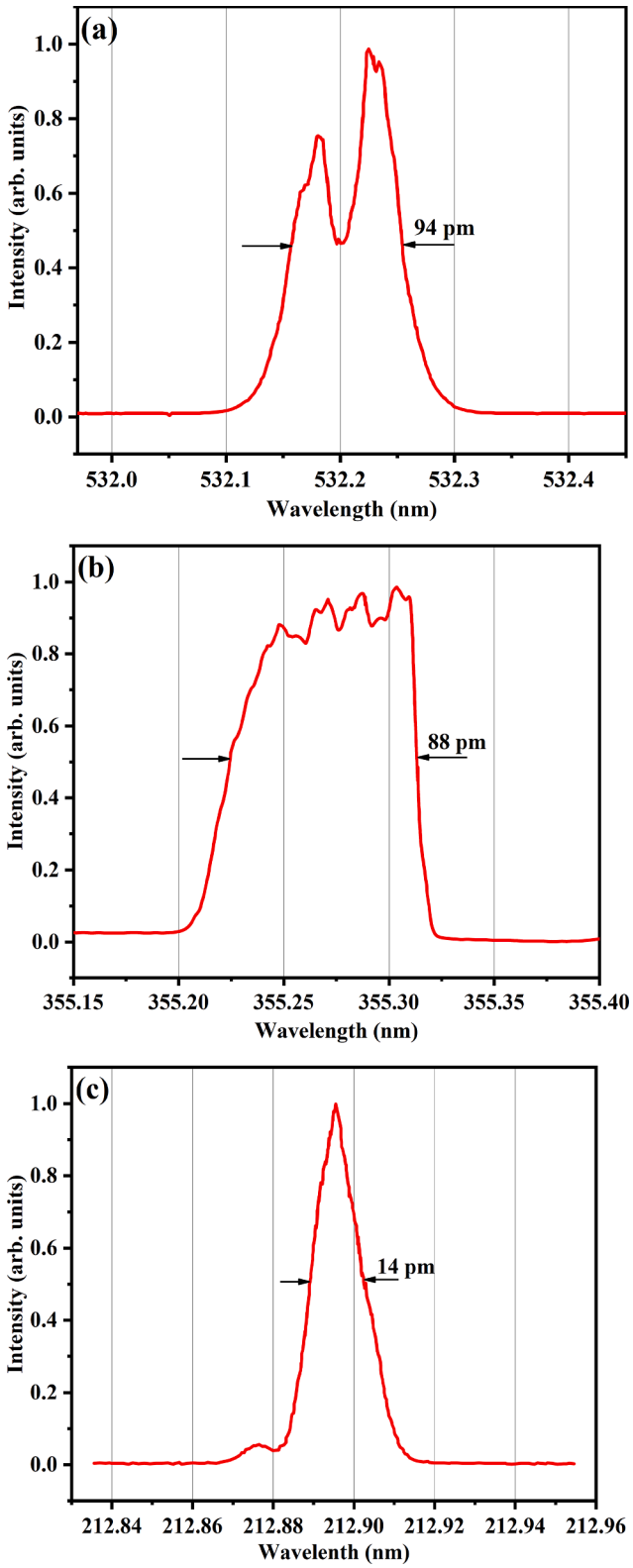

Fig. 5. Spectral evolution at (a) 532 nm, (b) 355 nm, and (c) 213 nm.

Finally, the long-term operation is investigated. The laser warming time is about 20 min. The BBO crystal is heated to 60 °C in a clean, dry-nitrogen-purged chamber to avoid hygroscopic deterioration and the formation of ozone. Although no surface degradation is observed, bulk optical degradation of BBO crystal after long-term generation of high-power radiation at 1.37 W is observed. The characteristic time of degradation varies from tens of hours using different BBO crystals. Then, we perform a 100-hour lifetime test of continuous operation at an 800 mW average output power as shown in Fig. 6. During 100-hour of operation, the same spot for the BBO crystal is used. There is no obvious power down. As we know, this is the longest lifetime reported for 800-mW levels at picosecond 213 nm no intermittent crystal shifting is required. The damage progress and the crystal degradation caused by TPA within the BBO crystal are effectively relieved by reducing the peak intensities of 532, 355, and 213 nm. No surface or internal damage is observed after the test, suggesting that the BBO crystal is a reliable NLO, which can be used to generate lasers with a 213-nm wavelength.

4 Conclusions

We have demonstrated a high-power picosecond deep ultraviolet laser generation system at 213 nm with a 1 MHz repetition rate in BBO crystals based on the "2 + 3" scheme. The maximum output power is as high as 1.37 W, which implies that the pulse energy is more than 1.3 μJ. Characteristics such as beam profiles, spectral evolution, and long-term operation are also investigated. A beam expander is used to reduce the TPA influence on BBO crystal and the divergence angle at 532 and 355 nm. The DUV system as a whole is found to operate for long periods at 800 mW without severe crystal degradation, and no requiring changes in crystal position. This design provides a good solution for a robust, long-term operation when operated at 213 nm due to the high reliability of the BBO crystal with accessible 532 and 355 nm beams.

Funding

National Science Foundation of China (NSFC) (61805174,

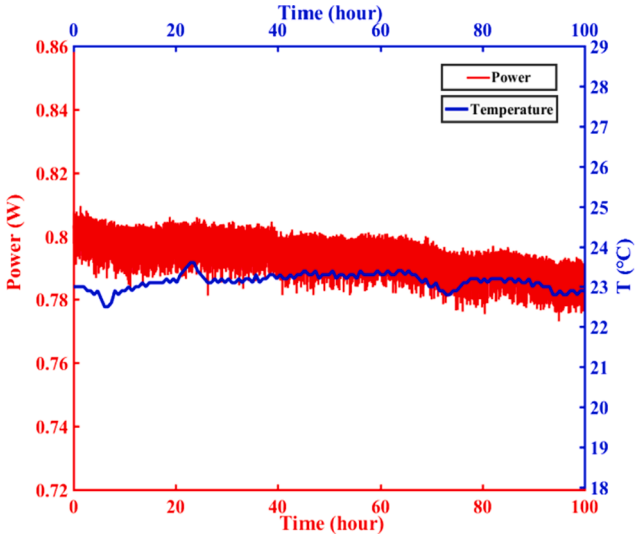

Fig. 6. Long-term 213-nm power stability of 100-hour lifetime test at 800 mW (red line), and the ambient temperatures T (blue line). (For interpretation of the references to colour in this figure legend, the reader is referred to the web version of this article.)

61535009, 61827821, 61377041, and 11527808);

Declaration of Competing Interest

None.

References

[1] A. Okamoto, H. Kuniyasu, T. Hattori, Detection of 0–40 nm particles on bulk -silicon and SOI wafers using deep UV laser scattering, IEEE Trans. Semicond. Manuf. 19 (2006) 372.

[2] B. Tan, Deep microhole drilling in a silicon substrate using multi-bursts of nanosecond UV laser pulses, J. Micromech. Microeng 16 (2006) 1.

[3] P.C. Gow, R.H.S. Bannerman, P.L. Mennea, C. Holmes, J.C. Gates, P.G.R. Smith, Direct UV written integrated planar waveguides using a 213 nm laser, Opt. Exp. 27 (2019) 29133.

[4] Y.K. Yap, M. Inagaki, S. Nakajima, Y. Mori, T. Sasak, High-power fourth- and fifth-harmonic generation of a Nd:YAG laser by means of a CsLiB6O10, Opt. Lett. 21 (1996) 1348.

[5] R. Wu, M.J. Myers, J.D. Myers, S.J. HaMlin, "560 mW, Fifth Harmonic (213nm), 200Hz Flashlamp Pumped Nd:YAG Laser System," in: S. Payne, C. Pollack (Eds.) Advanced Solid State Lasers, Vol. 1 of OSA Trends in Optics and Photonics Series (Optical Society of America, 1996), paper FC4.

[6] P. Zhu, D. Li, Q. Liu, J. Chen, S. Fu, P. Shi, K. Du, P. Loosen, 39.1 μJ picosecond ultraviolet pulses at 355 nm with 1 MHz repeat rate, Opt. Lett. 38 (2013) 4716.

[7] J. Sakuma, Y. Asakawa, T. Imahoko, M. Obara, Generation of all-solid-state, high-power continuous-wave 213-nm light based on sum-frequency mixing in CsLiB6O10, Opt. Lett. 29 (2004) 1096.

[8] Guozhu Chen, Hongxin Zou, Xiaokang He, Yong Shen, Qu Liu, "Fourth harmonic generation based on miniaturized tunable bow-tie resonators," Opt. Laser Technol. 114, 44 (2019).

[9] Pengfei Zhu, Chaomin Zhang, Kun Zhu, Yunxia Ping, Pei Song, Xiaohui Sun, Fuxin Wang, Yi Yao, 303 nm continuous wave ultraviolet laser generated by intracavity frequency-doubling of diode-pumped $P^{r3}+$:$LiY^{F}4$ laser, Opt. Laser Technol. 100 (2018) 75.

[10] I.A. Begishev, J. Bromage, S.T. Yang, P.S. Datte, S. Patankar, J.D. Zuegel, Record fifth-harmonic-generation efficiency producing 211nm, joule-level pulses using cesium lithium borate, Opt. Lett. 43 (2018) 2462.

[11] B. Köhler, T. Andres, A. Nebel, and R. Wallenstein, "High-power, high-repetition-rate fourth and fifth harmonic generation of a cw mode locked Nd: YVO4 laser," in: Conference on Lasers and Electro-Optics, OSA Technical Digest (Optical Society of America, 2000), paper CTuA8.

[12] K. Miyata, M. Mohara, K. Shimura, A. Tanabashi, L. Desbiens, V. Roy, Y. Taillon, S. Nakayama, S. Wada, Programmable deep-UV laser platform for inspection and metrology, Opt. Lett. 44 (2019) 5618.

[13] H. Turcicova, O. Novak, L. Roskot, M. Smrz, J. Muzik, M. Chyla, A. Endo, T. Mocek, New observations on DUV radiation at 257 nm and 206 nm produced by a picosecond diode pumped thin-disk laser, Opt. Exp. 27 (2005) 24286.

[14] B. Willenberg, F. Brunne, C.R. Phillips, U. Keller, "Efficient 2-W Average Power 206 nm Deep-UV Generation from 100-kHz Picosecond Pulses," in: Conference on Lasers and Electro-Optics, OSA Technical Digest (Optical Society of America, 2019), paper FTh1M.8.

[15] I.A. Begishev, R.A. Ganeev, A.A. Gulamov, E.A. Erofeev, Sh.R. Kamalov, T. Usmanov, A.D. Khadzhaev, Generation of the fifth harmonic of a neodymium laser and two-photon absorption in KDP and ADP crystals, Sov. J. Quant. Electron. 18 (1988) 224.

[16] Y. Mori, I. Kuroda, S. Nakajima, T. Sasaki, S. Nakai, New nonlinear optical crystal: cesium lithium borate, Appl. Phys. Lett. 67 (1995) 1818.

[17] C.T. Chen, B.C. Wu, A.D. Jiang, G.M. You, A new-type ultraviolet SHG crystal - beta-BaB_2O_4, Sci. Sin. 28 (1985) 235.

[18] https://www.spectronix-laser.com/products/2317/.

[19] Y. Orii, Y. Takushima, M. Yamagaki, A. Higashitani, S. Matsubara, S. Murayama, T. Manabe, I.Utsumi, D. Okuyama, G. Okada, "High-energy 266-nm picosecond pulse generation from a narrow spectral bandwidth gain-switched LD MOPA," in: Conference on Lasers and Electro-Optics, OSA Technical Digest (Optical Society of America, 2013), paper JTh2A.64.

[20] T. Sasaki, Y. Mori, M. Yoshimura, Progress in the growth of a $CsLiB_6O_{10}$ crystal and its application to ultraviolet light generation, Opt. Mater. 23 (2013) 343.

[21] I.A. Begishev, V.V. Ivanov, S. Patankar, P.S. Datte, S.T. Yang, J.D. Zuegel, J. Bromage, "Nonlinear Crystals for Efficient High-Energy Fifth-Harmonic Generation of Near-IR Lasers," in: Conference on Lasers and Electro-Optics, OSA Technical Digest (Optical Society of America, 2020), paper SW3E.2.

[22] M. Takahashi, A. Osada, A. Dergachev, P.F. Moulton, M.C. Raduban, T. Shimizu, N. Sarukura, Effects of pulse rate and temperature on nonlinear absorption of pulsed 262-nm laser light in β-BaB_2O_4, Jpn. J. Appl. Phys. 49 (2010), 080211.